



ELSEVIER

Global and Planetary Change 34 (2002) 153–171

GLOBAL AND PLANETARY
CHANGE

www.elsevier.com/locate/gloplacha

Calcification rate and temperature effects on Sr partitioning in coccoliths of multiple species of coccolithophorids in culture

Heather M. Stoll^{a,*}, Christine M. Klaas^{b,1}, Ian Probert^c,
Jorge Ruiz Encinar^d, J. Ignacio Garcia Alonso^d

^aDepartment of Geology, University of Oviedo, c/ Jesus Arias de Velasco, s/n, 33005 Oviedo, Spain

^bETH Zurich, Zurich, Switzerland

^cUniversity of Caen, Caen, France

^dDepartment of Analytical Chemistry, University of Oviedo, Oviedo, Spain

Received 10 July 2000; received in revised form 3 January 2001; accepted 19 January 2001

Abstract

Five common placolith-bearing coccolithophorid algae—*Gephyrocapsa oceanica*, *Coccolithus pelagicus*, *Calcidiscus leptoporus*, *Umbilicosphaera sibogae* (var. *sibogae* and var. *foliosa*), and *Emiliania huxleyi*—were cultured to investigate controls on Sr partitioning in coccolith calcite. For identical temperature and media composition, Sr partitioning varies by more than 30% in exponential phase cultures of the five species and is linearly related to rates of calcite production/cell ($\rho=0.91$). Exponential phase culture experiments with three strains of *C. leptoporus* and six strains of *G. oceanica* at varying temperatures show variations in Sr partitioning of 20% and 30%, respectively. With *C. leptoporus*, Sr partitioning is equally correlated with temperature and calcification rate ($\rho=0.8$), which themselves are highly correlated; the slope of the relationship between D_{Sr} and calcification rate is comparable to that observed in all species at constant temperature. However, in *G. oceanica*, increased temperature appears to enhance Sr incorporation by up to 2% to 1.6% °C⁻¹ in the range of 15 to 30 °C. The strong influence of calcification rate on Sr partitioning may be useful for inferring past variations in coccolithophorid productivity from Sr partitioning in coccolith sediments if the influence of temperature on Sr partitioning can be resolved. Because the relationship between calcite production and Sr partitioning is linear, a proportional change in calcification should be expressed much more strongly in the Sr/Ca ratio of large species with rapid calcite production than in smaller species, which produce calcite more slowly. Consequently, it may be possible to separate temperature and calcification influences on coccolith Sr/Ca by separately analyzing Sr/Ca in species that produce calcite rapidly and those that produce calcite slowly, if both undergo comparable relative changes in calcification rates.

© 2002 Elsevier Science B.V. All rights reserved.

Keywords: coccoliths; coccolithophorids; strontium; Sr/Ca; paleoceanography; climate change

* Corresponding author.

E-mail addresses: heather.stoll@asturias.geol.uniovi.es (H.M. Stoll), cklaas@starbuck.uchicago.edu (C.M. Klaas), Billard@ibba.unicaen.fr (I. Probert), ruizencinar@yahoo.com (J. Ruiz Encinar), jiga@sauron.quimica.uniovi.es (J.I. Garcia Alonso).

¹ Now at the Department of Earth Sciences, University of Chicago, Chicago, IL, USA.

1. Introduction

Coccolithophorid algae are commonly regarded as the main producers of calcium carbonate in open ocean settings (e.g., Takahashi, 1994; Westbroek et al., 1994; Riegman et al., 1998; Archer et al., 2000), and con-

sequently play important roles in the ocean's carbon and carbonate cycles. Coccolithophorids are also the only marine primary producers that leave a widespread fossil record: the coccoliths, or external plates of calcite, produced by these organisms enjoy long-term preservation above the carbonate compensation depth (CCD) worldwide. Consequently, the geochemical record preserved in coccolith calcite may provide a unique perspective on past changes in the carbon and carbonate cycle.

While the minor and trace element chemistry of foraminiferal calcite has been widely studied and used in paleoceanographic studies for over a decade, the minor element chemistry of coccolith calcite has been investigated only recently. A field study in the Equatorial Pacific suggested that the Sr/Ca ratio of coccoliths may be related to the calcification and growth rates of coccolithophorids (Stoll and Schrag, 2000). Because Sr/Ca ratios of seawater vary by less than 2% globally, the observed Sr/Ca variations of ~20% must reflect variations in Sr partitioning in coccolith calcite. The relationship between Sr partitioning in coccoliths and their calcification rates is consistent with control of Sr partitioning by calcification rate in abiogenic calcites (Lorenz, 1981). Such a relationship, if confirmed by further studies, could prove a valuable tool for investigating past changes in coccolithophorid productivity and their relation with past variations in climate and the carbon cycle. In particular, coccolith Sr/Ca may be useful to reconstruct past variations in the rain ratio of organic and carbonate carbon, hypothesized to be an important factor in glacial/interglacial atmospheric PCO_2 cycles (Archer et al., 2000). In addition, it is possible that coccolith Sr/Ca might be useful in correcting for growth rate effects on carbon isotope fractionation in coccolithophorid biomarkers, to improve estimates of past dissolved CO_2 concentrations in surface waters. However, in order to apply with confidence the intriguing relationships between Sr/Ca and calcification rate suggested by the field data, further investigation is needed. Culture studies represent an important context in which to investigate controls over minor element chemistry in coccoliths, because growth and calcification rates, along with calcification temperature, can be more reliably measured for comparison with geochemical data. In addition, these relationships can be evaluated for individual species, which has not yet been possible in sediment samples.

In this work, we present results of culture studies with five species of coccolithophorids algae with the aim of elucidating the controls of Sr partitioning in coccoliths. The relationships between C-isotope fractionation in coccolithophorids and Sr partitioning in coccoliths is being investigated in a separate and concurrent study (e.g. Stoll et al., 2002a) and are not presented here.

Nearly all previous culture studies of coccolithophorids have focused on a single species, *Emiliania huxleyi*. In part, this is because only *E. huxleyi* and its close relative *Gephyrocapsa oceanica*, produce alkenone biomarkers. The undersaturation ratio of these biomarkers (U_{K37}) is widely used in paleotemperature reconstructions (Prahl and Wakeham, 1987), and carbon isotopic fractionation in alkenones is used to reconstruct past dissolved PCO_2 concentrations in ocean surface waters (Jasper and Hayes, 1990; Jasper et al., 1994). In addition, culture studies of *E. huxleyi* have been extensively used to study coccolithophorid ecology, because *E. huxleyi* occurs widely throughout the modern ocean, is known to form large seasonal blooms, especially in the North Atlantic, and has been relatively easy to maintain in culture. However, since *E. huxleyi* is one of the smaller coccolithophorids and has a low coccolith weight, it is rarely a significant fraction (>10%) of coccolith calcite in sediments (Broerse, 2000). Consequently, in order to interpret the chemistry of coccoliths in ocean sediments on the basis of culture studies, it is critical to investigate the species that dominate coccolith carbonate in marine sediments. Significant contributors to coccolith carbonate in sediments are *Coccolithus pelagicus* at high latitudes, and *G. oceanica* and *Calcidiscus leptoporus* at low latitudes (Young and Ziveri, 2000). In this work, we present results on the chemistry of coccoliths from cultures of *G. oceanica*, *C. pelagicus*, *C. leptoporus*, *Umbilicosphaera sibogae* (var. *sibogae* and var. *foliosa*), and *E. huxleyi*.

Since calcification rates may be an important control on Sr partitioning in coccoliths, we first describe calcite production rates in three strains of *G. oceanica* at different temperatures, and one strain of *C. leptoporus* at a single temperature. We also present basic calcite production data for the other species. This data enables us to compare Sr partitioning with calcite/cell and coccolithophorid calcification

rates, in addition to culture temperature and cell division rates. We determine Sr partitioning in coccoliths for the five different species of coccolithophorids grown in similar culture conditions, in coccoliths from six strains of *G. oceanica* cultured at different temperatures and nutrient concentrations, and in coccoliths from three strains of *C. leptoporus* cultured at different temperatures. This dataset provides a reasonably coherent perspective on controls of Sr partitioning in coccolith calcite.

1.1. Kinetic and thermodynamics of Sr substitution in calcite

Kinetic effects strongly influence Sr incorporation in abiogenic calcites. Increasing the calcite precipitation rate over two orders of magnitude results in a five-fold difference in the effective Sr partitioning coefficient (Lorens, 1981; Tesoriero and Pankow, 1996). Watson (1996) attributed this dependence to surface enrichment effects during crystal growth, while Morse and Bender (1990) invoke surface reaction kinetics in general.

Thermodynamic effects on Sr incorporation in calcite cannot be established. Because Sr^{2+} has a larger ionic radius than Ca^{2+} , Sr forms a solid solution series with the orthorhombic aragonite structure rather than the rhombohedral calcite structure. Consequently, Sr substitution in calcite is very limited and deviates significantly from ideal solid solution behavior (Tesoriero and Pankow, 1996). Sr substitution in calcite is best described as ion camouflage phenomena rather than true solid solution; consequently, thermodynamic laws cannot predict equilibrium partitioning.

1.2. Ecology of coccolithophorid species studied

All of the five species cultured in this study form heterococcoliths, radial arrays of complex-shaped crystals of calcite, whose final morphologies are placoliths, two disc-like shields connected by a tube. All heterococcoliths are produced intracellularly and are subsequently passed through the cell membrane, forming a continuous covering around the cell (see deVrind-deJong et al., 1994; Young et al., 1999 for a detailed discussion of calcification in coccolithophorids). In some of the culture experiments with *G. oceanica* and *C. leptoporus*, multiple layers of cocco-

liths are formed around the cell. In addition, coccoliths may be shed from the cell, especially during later growth stages as cell division rates cease, a phenomena especially common for *G. oceanica* and *E. huxleyi*.

Placolith-bearing forms generally dominate in areas of upwelling (coastal or open ocean) and coastal and shallow-sea assemblages. *G. oceanica* and *E. huxleyi* can form large seasonal blooms as well. All of these represent eutrophic environments in which rapid population growth can occur (Young, 1994).

2. Methods

2.1. Culture methods

To compare calcification and calcite chemistry of coccoliths under different environmental conditions, six strains of *G. oceanica* were cultured at ETH Zurich at temperatures ranging from 17 to 30 °C. Precision of measurements of culture temperatures is $\pm 0.65^\circ$. Three strains of *C. leptoporus* were cultured at temperatures ranging from 17 to 22 °C. *G. oceanica* strains were isolated from the warm, oligotrophic Gulf Stream off the coast of Miami (A 4725 and A 4727), and from more temperate areas in the Western Atlantic (PC71 and ARC3) and Mediterranean (JS8 and ESP 186). Details on all the strains and their location and date of collection are given in Appendix A. The strains were preadapted to experimental conditions for approximately nine generation periods before collection of samples or growth rate data. Sixty-milliliter batch cultures were grown in coastal seawater enriched in nutrients, vitamins, and trace metals. Most experiments were conducted with nutrient enrichment at $f/2$ levels, although some experiments were conducted at $f/20$ and $f/200$ nutrient levels (Guillard, 1975); nutrients were always in excess during logarithmic growth phase. Cultures were maintained in light-saturating conditions ($175 \pm 25 \mu\text{E m}^{-2} \text{s}^{-1}$) on a 14 h light/10 h dark cycle. Cultures were semicontinuous, maintained in the log growth phase via frequent transfers, and samples were always collected in log-phase except where noted. Cultures were grown in Erlenmeyer flasks with cotton stoppers to maintain air-media CO_2 exchange but prevent bacterial invasion. Frequent cell density measurements with a haemocy-

tometer permit precise calculation of log growth rates for each culture experiment. For each strain at each culture conditions, the length and width of the coccosphere were also measured as part of a study on morphometrics (Klaas et al., in preparation).

To compare chemistry of coccoliths of different species under similar environmental conditions, a single strain each of *E. huxleyi*, *G. oceanica*, *C. pelagicus*, *C. leptoporus*, *U. sibogae sibogae*, and *U. sibogae foliosa* were cultured at the University of Caen. Three-hundred-milliliter batch cultures were grown in filter-sterilized coastal seawater enriched in nutrients, vitamins, and trace metals to standards for K/2 medium (Keller et al., 1987); nutrients were always in excess during logarithmic growth phase. Cultures were grown at 17 °C (acclimated as above) in light saturating conditions on a 14:10 LD cycle. Cultures were initiated in log phase and were sampled multiple times in both log and stationary phase over a 2- to 3-week period. Cell density and culture medium pH were measured at each sampling point. Cell diameter and coccosphere diameters were also measured for cells in exponential phase (Table 1). Log phase growth rates are calculated from cell density changes between sampling intervals. Because of the large range in cell sizes in different species, in addition to cell division rate, is it also useful to estimate the rate of organic C uptake by the cells, equivalent to the organic C quota of the cell times the cell division rate. If we assume that C quota is proportional to biovolume (reasonable for the small cell sizes of these algae where vacuoles are not important (H. Kinkel, personal communication, 2000)), it is possible to estimate carbon quotas from the biovolume of these cells. We calculate pg organic

C/biovolume relationships from experiments with *E. huxleyi*, indicating typical cell quotas of 20 pg organic C/cell with cell diameters of approximately 4 µm (Fernandez et al., 1996).

2.2. Measuring coccolith chemistry

From cultures at ETH, a variable amount of culture was centrifuged to concentrate cells. The pellet was rinsed in distilled water and dried at 50 °C. Harvested samples in most cases represent a composite sample from three replicate cultures grown in parallel. In some of the experiments at 17 °C, samples from the three replicates were harvested and analyzed separately. In preparation for Sr/Ca analysis, samples of 40–80 µg carbonate were briefly sonicated then centrifuged with the following series of rinses: ethanol, acetone, methanol, 0.001 N HNO₃, and distilled water. Differences in Sr/Ca for cleaned and noncleaned replicates were indistinguishable from analytical uncertainty since no major contaminant phases significantly affect carbonate Sr/Ca ratios. Organic fractions do not contain significant Sr or Ca relative to carbonates and seawater Sr/Ca ratios are similar to carbonate Sr/Ca ratios. Subsequently, samples were dissolved in 200 µl of 2% ultrapure HNO₃.

For cultures at Caen, 10 ml of culture was centrifuged down to concentrate cells, except for the first sampling of each culture (Day 3) where a larger but unrecorded culture volume was sampled. The pellet was rinsed twice in distilled water and dried at 50 °C. Prior to splitting for analysis of calcification and Sr/Ca ratios, the samples were rinsed in ethanol and methanol. For Sr/Ca measurements, samples were rinsed again in ethanol and distilled water (with pH adjusted to 8.5 with NH₄OH) prior to dissolution in 50 µl of 2% ultrapure HNO₃.

Sr/Ca was measured via inductively coupled plasma-mass spectrometry (ICP-MS) on a Finnigan ELEMENT sector field instrument in the Department of Analytical Chemistry at the University of Oviedo. Ratios were measured in pulse-counting mode on dilute solutions (10 ppm Ca). Matrix-matched standards were used to correct for mass bias and detector dead time. Precision of the analyses is better than 0.4% relative standard deviation (rsd).

Table 1
Cell and coccosphere sizes from Caen cultures (17 °C)

Species	Cell diameter (µm)	Coccosphere diameter (µm)	pg calcite/cell
<i>E. huxleyi</i> (MS1)	3.48	5.44	28
<i>G. oceanica</i> (JS1A)	5.09	7.47	186
<i>C. leptoporus</i> (PC11M2)	11.34	16.25	1600
<i>C. pelagicus</i> (KL2)	14.11	16.25	836
<i>U. sibogae sibogae</i> (ASM36)	7.11	25.01	252
<i>U. sibogae foliosa</i> (ESP6 M1)	8.75	12.63	398

2.3. Measuring calcification

Calcite production was monitored throughout log phase growth in several of the ETH culture experiments. Five to ten milliliters of well-mixed culture solution were filtered onto a 25 mm polycarbonate filter. The filter was well rinsed with buffered distilled water to remove seasalts and dried. Filters were acidified to dissolve calcium carbonate, and the concentration of Ca was measured via flame atomic absorption spectroscopy on a Pye-Unicam SP9 instrument in the Department of Geology at the University of Oviedo. Precision of the Ca measurement is better than 2% (rsd), based on replicate analyses of the same sample. However, precision of the overall measurement of calcite production averages 7% (rsd) based on analysis of replicate samples collected from the culture on the same day. This latter precision is of the same order of magnitude as for cell counts, suggesting that variation may result from inhomogeneous distribution of cells in a small subsample of the culture. Because rigorous cleaning was not necessary for Sr/Ca measurements, we were also able to measure Sr/Ca ratios of some of the coccolith samples dissolved from polycarbonate filters.

Calcite production was estimated in samples cultured at Caen by suspending the harvested coccolith pellet in 1 ml of ethanol and extracting an aliquot of 50 μ l. This carbonate was dissolved in acid and the Ca concentration was also measured via flame atomic absorption spectroscopy. These estimates are less precise than those for the ETH cultures, given greater uncertainty in the volume of culture harvested, and the possibility of inhomogeneous distribution of carbonate when the sample suspension was split.

Like all commonly used methods for measuring calcification rates and calcite production (e.g. ^{14}C incorporation, filter weight, etc.), these measurements are independent of whether the coccoliths are attached to the cells or loose in the media. While these methods measure net, rather than gross, calcite production, redissolution of calcite in the media is generally believed to be minor. Our measurements represent integrated calcification rates over a period of up to several days. However, “instantaneous” calcification rate determinations (via ^{14}C incorporation) and determinations of integrated calcite production in previous culture experiments with *E. huxleyi* are consistent and

suggest rather continuous calcite production during the photoperiod (e.g. Nimer and Merrett, 1992; Dong et al., 1993).

3. Calcite production in coccolithophorids

3.1. Comparing calcification in *G. oceanica* under different culture conditions

G. oceanica strains cultured at ETH produce between 50 and 400 pg calcite/cell. The calcite produced in each culture experiment is plotted as a function of cell density in Fig. 1. In Gulf Stream strains A4725 and A4727 (Fig. 1a), calcification is relatively constant with increasing cell density (Fig. 1a). For these strains, there is a consistent increase in calcification with temperature (Fig. 1b).

The temperate *G. oceanica* strain ARC3 produces more calcite per cell than the tropical strains, a maximum of 400 pg/calcite per cell, and exhibits decreasing calcification per cell at higher cell densities (Fig. 1c). Upon transfer from a dense culture to a new culture, calcite production increases rapidly. The decrease in calcification at higher cell densities likely results from a more rapid drawdown of Ca (and alkalinity) in the media of these high-calcifying temperate strains compared to the lower-calcifying tropical strains, combined with the higher overall cell densities reached in the high-calcifying cultures. However, it is possible that this is not truly a decrease in calcite production but an increase in the dissolution of calcite, perhaps of loose coccoliths, in the media. Brownlee et al. (1994) showed that in *E. huxleyi*, calcification rates decreased with decreased concentrations of Ca^{2+} in media. In Fig. 1d, we plot, for all strains and temperatures, the μg calcite/ml of culture media, proportional to the drawdown of Ca^{2+} in the culture. All strains show a change in slope of calcite production vs. cell number at 60 μg of calcite/ml. Since for a given cell density, ARC 3 strains have higher drawdown of alkalinity than A4727 and A4725 strains, the tendency of decreasing calcification with higher cell densities is more pronounced.

Given the change in calcification with cell density, it is more difficult to compare calcite production under different culture conditions for the ARC3 strains. Fig. 1c suggests that calcite production is

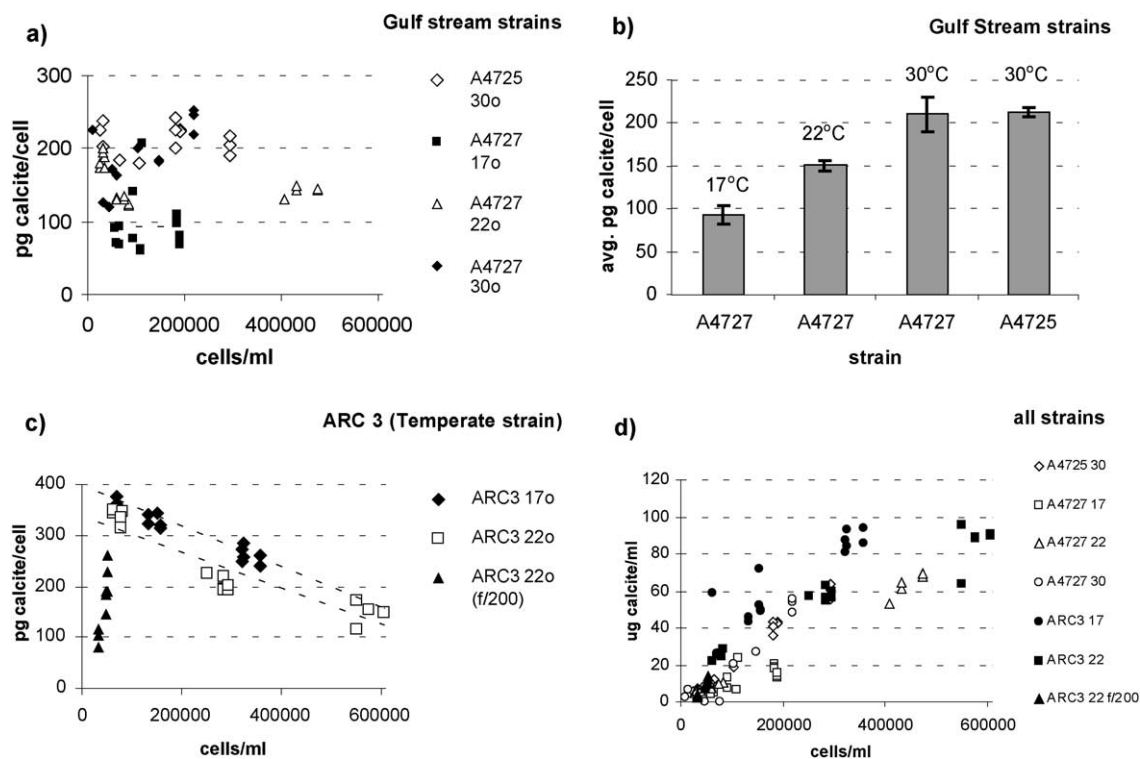


Fig. 1. Calcite production in *G. oceanica* strains cultured at ETH. (a) pg calcite/cell for Gulf stream strains A4725 and A4727 plotted vs. cell density. (b) Average pg calcite/cell for *G. oceanica* Gulf Stream strains A4725 and A4727. Average of all experiments run for that strain at a given temperature; error bars are the standard error of the mean. (c) pg calcite/cell vs. cell density for ARC 3 strains grown at different temperature and nutrient conditions. Trendlines are given for 17 and 22 °C experiments at *f/2* nutrient levels. Equation for 17 °C experiment is $y = -3.98 \times 10^{-4}x + 3.98 \times 10^2$; for the 22 °C experiment is $y = -3.54 \times 10^{-4}x + 3.92 \times 10^2$. (d) μg of calcite/ml culture volume vs. cell density for all *G. oceanica* calcite production data from ETH cultures. Open symbols indicate Gulf Stream strains with relatively constant calcification/cell with increasing cell density, whereas solid symbols indicate higher-calcifying temperate strain ARC3, which exhibits decreasing calcite/cell with increasing cell density.

lower for the 22 °C conditions than the 17 °C conditions by ~ 40 pg calcite/cell. We calculate an average of 338 and 361 pg calcite/cell, respectively, for cultures with cell densities in the range of 60,000 to 80,000 cells/ml (where maximum calcification is obtained). A linear curve fit yields y -intercepts of 398 and 339, respectively. Given that cell densities for the *f/200* experiment do not overlap with the other experiments, it is not possible to compare calcite production.

For both Gulf Stream and temperate strains, there is a strong positive relationship between pg calcite/cell and coccospere length and coccospere surface area (Fig. 2). This relationship could be controlled by cell size, where larger cells have a greater surface area to

cover with calcite. However, in these cultures, *G. oceanica* in many cases added multiple layers of cocoliths, so most likely that the correlation between larger coccospere (and larger coccospere surface area) and higher calcite/cell results from multiple layers of cocoliths. This linear relationship between pg calcite/cell and coccospere surface area shows a consistent slope between the temperate and Gulf Stream strains despite differences in their ecology. The consistency between coccospere size and calcite/cell suggests either that loose cocoliths are not a significant fraction of the calcite in the culture, or that their proportion is comparable in these experiments.

Estimates of calcite/cell, combined with data on cell division rates, permit calculation of calcification

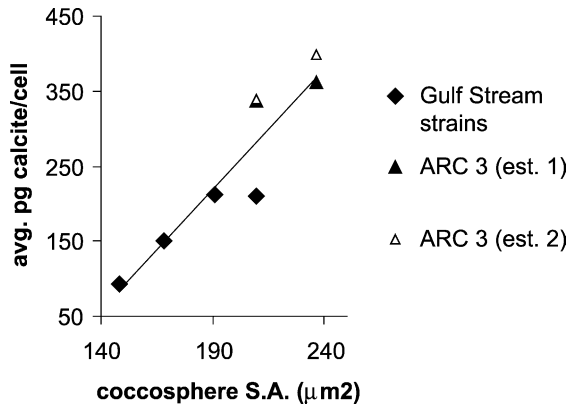


Fig. 2. Relationship between average pg calcite/cell and coccosphere surface area for *G. oceanica* strains cultured at ETH. For ARC3 strains, calcification is estimated for cell densities of 60,000 to 80,000 cells (est. 1) and by the y-intercept in Fig. 1c (est.2).

rates for these *G. oceanica* experiments. Because calcification rates may be an important control of Sr partitioning in coccolith calcite, it is desirable to estimate calcification rates for all strains and experimental conditions since Sr partitioning was measured in many more experiments than calcification. On the basis of the observed relationships between coccosphere diameter and calcite/cell in Fig. 2, we estimate calcite/cell of *G. oceanica* strains for experiments in which morphometric, but not calcification data, were collected. The most important caveat in this calculation is that *G. oceanica* can shed coccoliths, which could partially decouple the relationship between calcite production and coccosphere size. In addition, relationships between coccosphere size and calcification could be altered if some changes in coccosphere size are due to changes in cell size whereas others reflect merely changes in number of coccolith layers. Due to the very large coccosphere dimensions of some of the temperate strains at the highest temperatures, estimated calcification for some experiments is as high as 1000 pg calcite/cell. For these experiments, which fall far from the range of calibrated surface area/calcite relationship, we assume a large uncertainty in subsequent discussions (and indicate these with error bars of $\pm 25\%$ in subsequent figures). For strains where calcite/cell is likely to decrease with increasing cell density, the estimated calcite/cell represents a maximum calcite/cell and the calcification

rate a maximum calcification rate. Because of these uncertainties, data on calcification rates estimated from morphological data are distinguished by different symbols in subsequent figures.

3.2. Comparing calcification in other species under similar culture conditions

Replicate experiments of *C. leptopus* strain PC11 M2 (17 °C) cultured at ETH have much higher calcification per cell than *G. oceanica*, consistent with the larger cell diameter and coccosphere diameter of this species and the greater amount of calcite per coccolith. *C. leptopus* cultures show a strong trend towards decreasing calcification with increasing cell density (Fig. 3a), presumably due to the very high degree of calcification and subsequent depletion of

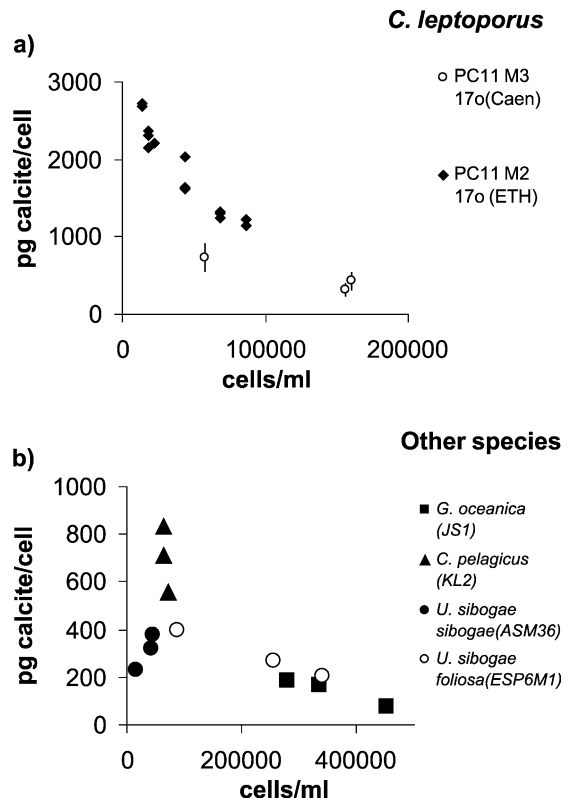


Fig. 3. Calcite production in other coccolithophorid species cultured at Caen. (a) pg calcite/cell vs. cell density for *C. leptopus* at 17 °C. (b) pg calcite/cell vs. cell density for *C. pelagicus*, *G. oceanica* (JS1), *U. sibogae* sibogae, and *U. sibogae* foliosa, at 17 °C.

media Ca^{2+} . This trend is also observed in strain PC11 M3 (17 °C) cultured at Caen, although this strain appears to calcify to a lesser extent than PC11 M2.

Other species cultured at 17 °C at Caen show variable degrees of calcification, from 23 pg calcite/cell for *E. huxleyi* to over 800 pg calcite/cell for *C. pelagicus* (Fig. 3; *E. huxleyi* not plotted). Temperate *G. oceanica* strain JS1 shows similar calcite production to temperate *G. oceanica* strain ARC 3 discussed previously, with similar decreases in calcification with increasing cell density. Calcification in *U. sibogae sibogae* and *U. sibogae foliosa* is comparable to that in *G. oceanica*, ranging from 400 to 50 pg calcite/cell and exhibiting similar decreases with increasing cell density.

For some of the experiments with *C. leptoporus* carried out at ETH, neither morphometric nor calcification data were collected. For these experiments, we have used the data from *C. leptoporus* PC11 M2 (17 °C) to estimate calcite/cell and maximum calcification rates, indicating on figures the greater uncertainty in these estimates. For Caen cultures, calcification rates could be calculated only for exponential phase cultures where cell division rates are calculated.

4. Sr partitioning in coccolith calcite

4.1. Calculation of Sr partitioning coefficients

In this study, we seek to distinguish how Sr partitioning in coccoliths responds to different culture conditions. Hence, in measuring coccolith Sr/Ca, we wish to distinguish variations due to differences in media Sr/Ca ratio from those due to differences in Sr partitioning. The Sr/Ca ratio of the stock media is essentially constant since there is very little variation in seawater Sr/Ca ratios and since seawater for culture media is collected in large batches, which are well mixed. However, in these batch cultures, cell densities are higher than those typically encountered in natural ocean settings, and production of calcite by coccolithophorids can progressively elevate media Sr/Ca ratios since coccolith calcite production fractionates against Sr. Media samples taken from the cultures were not appropriately preserved to permit direct measurement of media Sr/Ca (media

samples were not filtered so calcite had redissolved). However, from measurements of calcification, it is possible to calculate the media Sr/Ca ratios. For most of the cultures, calcite production enriches the media only slightly in Sr, although for some high calcifying strains, Sr/Ca ratios may increase by several percent.

Here we calculate an effective Sr partitioning coefficient based on the calculated Sr/Ca ratio of the media, although the Sr/Ca ratio of the intracellular calcifying fluid could differ from seawater if cellular uptake mechanisms fractionate Ca and Sr. Because calcite is produced continuously and media Sr/Ca is changing, each increment of calcite is produced from media with a slightly different Sr/Ca ratio. Consequently, to calculate the average effective Sr partitioning coefficient (D_{Sr}) of a given coccolith sample, we calculate the average media Sr/Ca ratio weighted by the amount of calcite produced at each media composition:

$$D_{\text{Sr}} = \frac{(\text{Sr/Ca coccolith calcite})}{(\text{weighted mean Sr/Ca media})}$$

Weighted average media composition is solved in a spreadsheet by calculating the amount of coccolith calcite produced for each increase in cell density, based on the amount of calcite/cell measured/estimated from the calcification studies. The calculation is solved in increments of 2000 cells/ml and accounts for decreasing calcification with increased cell densities in some strains. From the amount of calcite produced and a hypothetical Sr partitioning coefficient, we calculate the change in Sr/Ca ratio of the media for each increase in cell density. We then calculate the average media Sr/Ca at which the culture grew, weighted by the amount of calcite produced at each media composition. Because the model is relatively insensitive to the exact value chosen for the Sr partitioning coefficient, we are able to run it using the measured Sr/Ca ratio for each sample. Because of uncertainties in estimating calcification for each culture, calculation of Sr partitioning coefficients carries additional uncertainty, which we estimate at less than 1% for *G. oceanica*. In all subsequent figures, the partitioning coefficient shown has been corrected for changes in media Sr/Ca. A vertical bar indicates the difference between partition-

ing coefficients calculated with and without correcting for changes in media Sr/Ca, illustrating that the variability in media composition is insignificant for most samples.

For some of the experiments with *C. leptoporus* carried out at ETH, neither morphometric nor calcification data were collected. For these experiments, we have used the data from *C. leptoporus* PC11 M2 (17 °C) and illustrate the D_{Sr} without correction for media composition (upper error bar), and assuming calcification/cell double that of *C. leptoporus* PC11 M2 (17 °C) (lower error bar).

Because this model calculates iteratively the amount of calcite produced by cells, accounting for decreasing calcite/cell in some experiments, we also use it to calculate the average calcification rate for the experiments. Average calcification rate differs from the maximum calcification rate only for experiments where calcite/cell decreases with increasing cell density.

4.2. Sr partitioning in different species at 17 °C

Where harvested separately, samples from replicate cultures of *G. oceanica* at ETH showed similar Sr partitioning coefficients (relative standard deviation (rsd) of 1.6%). Because morphometric measurements used to estimate calcification for many strains are available only for the composite sample, we use the average Sr partitioning coefficient and growth rate for these replicate samples for subsequent figures and statistical calculations.

Sr partitioning coefficients for different species cultured at 17 °C range from 0.257 to 0.356, a variation of 32% (data given in Appendix B). Among the different species, D_{Sr} is not correlated with cell division rate (Fig. 4a). However, for the Caen cultures where we could estimate the rate of C incorporation/cell/day (as described in Section 2.1), D_{Sr} is highly correlated with growth rates expressed in terms of C uptake rather than cell division (Fig. 4b; $\rho=0.94$). D_{Sr} is also highly correlated with the average calcification rate (Fig. 4c; $\rho=0.91$), since calcite production/cell also varies with cell and coccosphere size (Table 1).

Slight decreases in D_{Sr} are observed through the growth stage of the culture (Fig. 5a), ranging from 3% in *C. pelagicus*, *C. leptoporus*, and *U. sibogae*

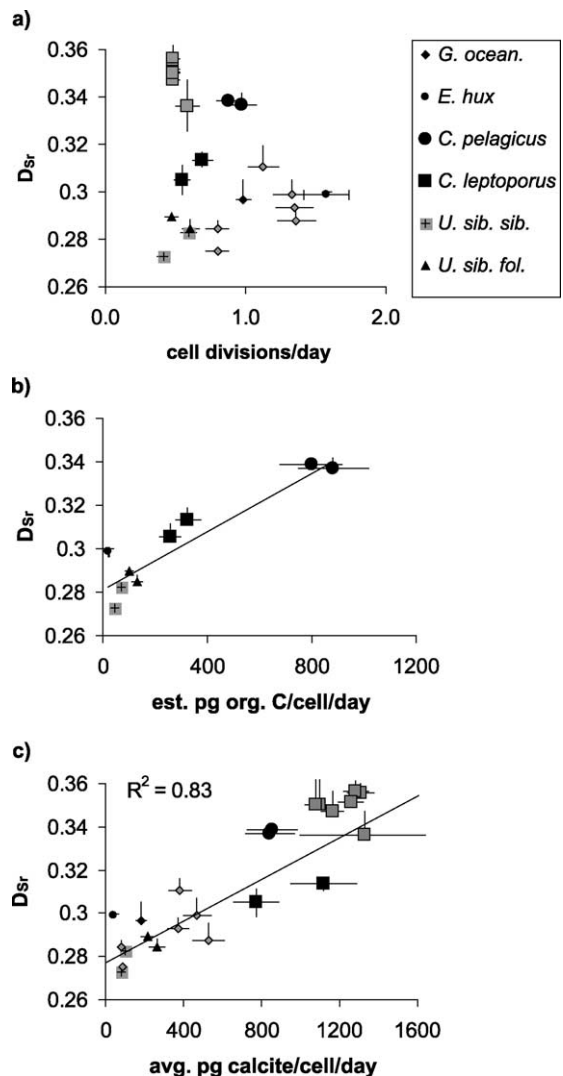


Fig. 4. D_{Sr} vs. cell division rate and calcification rate for all exponential phase cultures at 17 °C. Upper vertical error bars indicate magnitude of correction for changes in media Sr/Ca, as described in the text (Section 4.1). Where calcification rates were not measured or estimated from morphometric data, lower vertical error bars are given, as described in the text (Section 4.1). (a) D_{Sr} vs. cell division rate; horizontal error bars indicate $\pm 10\%$ uncertainty in cell division rates. (b) D_{Sr} vs. estimated organic C fixation rate; horizontal error bars show $\pm 15\%$ uncertainty. (c) D_{Sr} vs. calcification rate; horizontal error bars indicate $\pm 5\%$ uncertainty where calcification and Sr/Ca were directly measured from polycarbonate filters; $\pm 25\%$ uncertainty where calcification was not measured and no morphometric data were available; and $\pm 15\%$ for all other cases. Equation for regression line is $y = 5.56 \times 10^{-5}x + 0.278$.

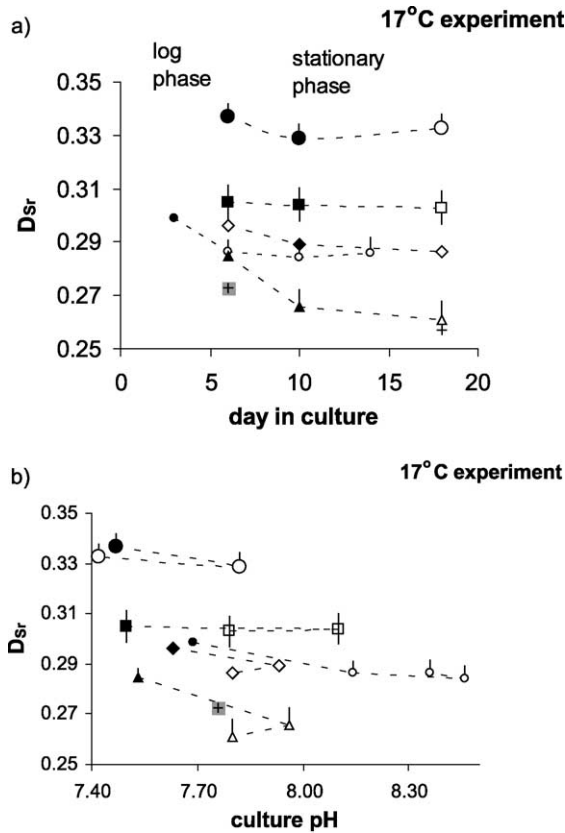


Fig. 5. (a) For Caen cultures, changes in D_{Sr} in different species over the course of the culture period. (b) For Caen cultures, changes in D_{Sr} in different species as a function of changes in media pH over the course of the culture period, with dashed lines connecting consecutive samples. In both (a) and (b), solid symbols indicate growth in exponential phase, open symbols indicate stationary phase. Symbol shape corresponds to different species as in Fig. 4.

sibogae, 5% in *G. oceanica* and *E. huxleyi*, and 10% in *U. sibogae foliosa*. These decreases could correspond to slowing calcification rates in late log phase and in stationary phase; we can only estimate calcification rates for purely log phase samples. Changes in culture media may also contribute to changing Sr partitioning. Culture media was initially pH 7.65, but in many cultures pH later approached or exceeded 8.0. Decreases in D_{Sr} in *E. huxleyi* correspond to increases in pH; however, D_{Sr} is relatively stable in *C. leptoporus* despite even larger changes in media pH (Fig. 5b). Furthermore, while D_{Sr} generally decreased slightly

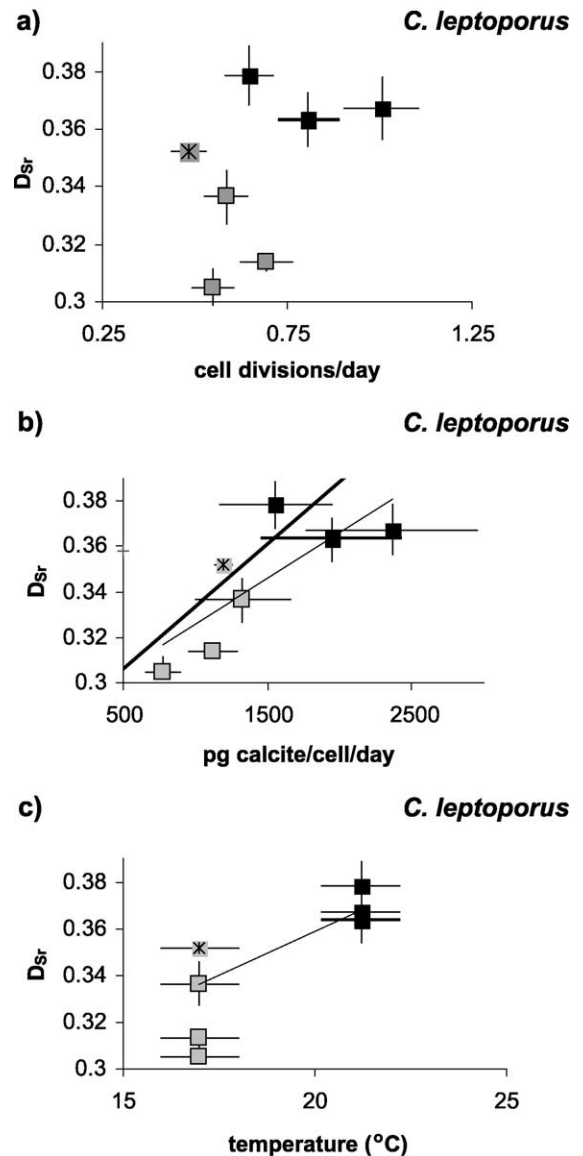


Fig. 6. *C. leptoporus* cultures, D_{Sr} vs. cell division rate (a), D_{Sr} vs. calcification rate (b), and D_{Sr} vs. temperature (c). Solid black symbols indicate samples cultured at 22 °C, other symbols cultured at 17 °C; squares with star pattern at center distinguish samples collected on polycarbonate filters for which we have precise estimates of calcification rates. In (b), bold trendline shows best fit of calcification rate vs. D_{Sr} for all species at 17 °C from Fig. 4; thin line shows best fit for *C. leptoporus* data at all temperatures ($y=4.02 \times 10^{-5}x+0.286$). In (c), the regression line is $y=6.38 \times 10^{-3}x+0.228$. Vertical and horizontal error bars for (a) and (b) are as described in Fig. 4. For (c), vertical error bars are as described in Fig. 4, horizontal error bars reflect 1 degree uncertainty in temperature control of cultures.

Table 2
Cross-correlations for *C. leptoporus*

	Temperature	Cell division/day	pg calcite/cell/day	pg calcite/cell	D_{Sr}
Temperature	1.00				
Cell division/day	0.83	1.00			
pg calcite/cell/day	0.87	0.87	1.00		
pg calcite/cell	0.19	-0.09	0.41	1.00	
D_{Sr}	0.83	0.47	0.79	0.93	1.00

throughout the growth period, pH in many cultures increased during exponential phase but then decreased later in stationary phase. Media alkalinity may also have decreased due to calcification by as much as 1.4 mEq/l, but alkalinity increases due to NO_3^- removal in organic fractions cannot be readily calculated.

4.3. Sr partitioning in *C. leptoporus* under different culture conditions

At ETH, two strains of *C. leptoporus* were cultured at temperatures of 17 °C and 22 °C. Fig. 6 illustrates

the relationships between Sr partitioning and cell division, calcification rates, and temperature in these experiments, and cross-correlation statistics are given in Table 2. While growth rate, calcification rate, and temperature are all highly intercorrelated, D_{Sr} is most strongly correlated with calcification rate and temperature. The slightly weaker correlation with calcification rate as opposed to temperature may in part result from the high uncertainties of the calcification rate estimates for the 22 °C samples. In Fig. 6b, we show that the best fit line for the relationship between calcification and Sr partitioning in all species at constant temperature (bold line; equation in Fig. 4b) approximates well the trend in the *C. leptoporus* data, and falls within the 75% confidence intervals for the best fit line for the *C. leptoporus* data at both temperatures (thin line).

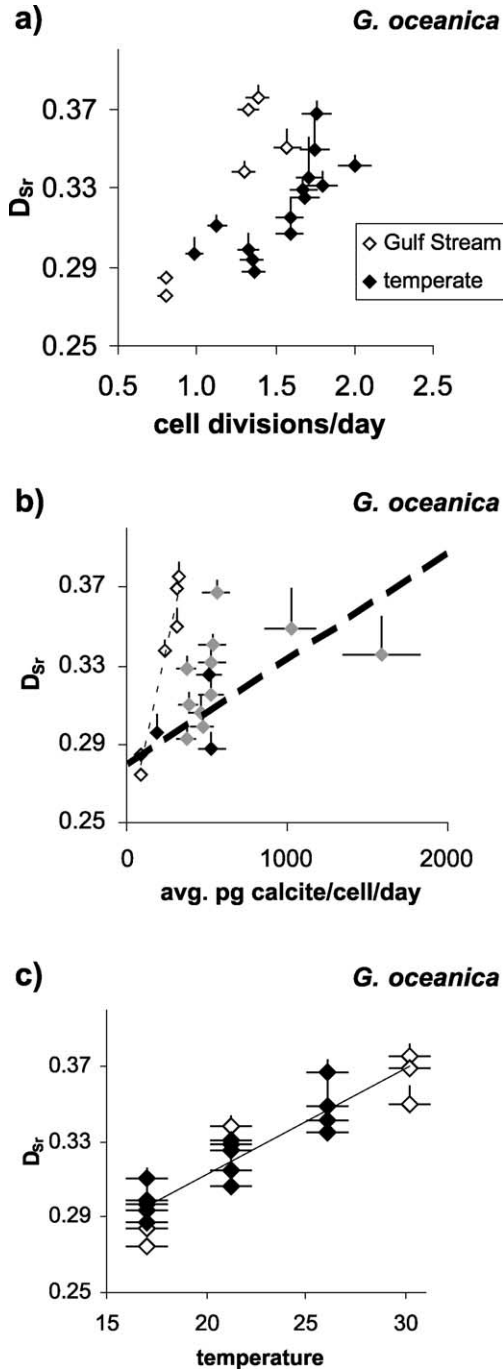
4.4. Sr partitioning in *G. oceanica* under different culture conditions

For the experiments with *G. oceanica* cultured at different temperatures, we distinguish the response of the Gulf Stream strains and temperate strains because

Table 3
Cross-correlations for *G. oceanica*

	Temperature	Cell division/day	pg calcite/cell/day	pg calcite/cell	D_{Sr}	max pg calcite/cell/day
<i>(A) G. oceanica, all strains</i>						
Temperature	1.00					
Cell division/day	0.60	1.00				
pg calcite/cell/day	0.38	0.61	1.00			
pg calcite/cell	0.34	0.51	0.97	1.00		
D_{Sr}	0.92	0.58	0.29	0.24	1.00	
max pg calcite/cell/day	0.35	0.62	1.00	0.96	0.27	1.00
<i>(B) G. oceanica, Gulf Stream strains</i>						
Temperature	1.00					
Cell division/day	0.91	1.00				
pg calcite/cell/day	0.97	0.97	1.00			
pg calcite/cell	0.89	0.94	0.88	1.00		
D_{Sr}	0.95	0.90	0.98	0.77	1.00	
<i>(C) G. oceanica, temperate strains</i>						
Temperature	1.00					
Cell division/day	0.86	1.00				
pg calcite/cell/day	0.64	0.48	1.00			
pg calcite/cell	0.48	0.31	0.98	1.00		
D_{Sr}	0.90	0.74	0.44	0.29	1.00	
max pg calcite/cell/day	0.65	0.49	1.00	0.97	0.45	1.00

they have different morphology and growth rate responses to temperature (Klaas et al., in preparation; Table 3). Overall, partitioning coefficients for Sr vary



from 0.275 to 0.376, a range of 31%. Sr partitioning coefficients are correlated with cell division rates overall and for both groups of strains individually (Fig. 7a ($\rho(\text{overall})=0.58$; $\rho(\text{Gulf stream})=0.90$; $\rho(\text{temperate})=0.74$). For Gulf Stream strains, where calcification was measured directly and does not vary with cell density, Sr partitioning and calcification rate correlate strongly ($\rho=0.98$; Fig. 6b). However, the slope of this relationship is much steeper than that observed between calcification rate and D_{Sr} in all species at constant temperature (Fig. 7b). For temperate strains, where calcification typically varied with growth rate and was in nearly all cases estimated from morphometry, D_{Sr} correlates more weakly with calcification rate ($\rho=0.45$). This latter statistic is dominated by the three outliers where the estimation of calcification rate may not be reliable; it is possible that the remaining data would define a steep trend parallel to that of the Gulf Stream strains. When the two strains are considered together, D_{Sr} correlates only weakly with calcification rate ($\rho=0.29$), and is most strongly correlated with temperature ($\rho=0.92$; Fig. 7c). For temperate strains, the correlation between D_{Sr} and temperature ($\rho=0.90$) is much greater than for either cell division rate or calcification rate. For Gulf Stream strains, the difference in correlation between D_{Sr} and temperature ($\rho=0.95$) and D_{Sr} and calcification (0.98) is not likely to be significant given the uncertainty in both measurements. Attempts to vary growth rate independent of temperature using varying nutrient concentrations were unsuccessful, as growth rates at lower nutrient levels were not significantly different from those at $f/2$ levels. In addition, some of the lower nutrient experiments were harvested at cell densities too low to yield sufficient carbonate for Sr/Ca analysis.

Fig. 7. *G. oceanica* cultures, D_{Sr} vs. cell division rate (a), D_{Sr} vs. calcification rate (b), and D_{Sr} vs. temperature (c). In (b), bold trendline shows best fit of calcification rate vs. D_{Sr} for all species at 17 °C from Fig. 4; thin dashed line shows best fit for *G. oceanica* (Gulf Stream strain) data at all temperatures ($y=3.71 \times 10^{-4}x + 0.248$). For (c), linear regression line is $y=5.63 \times 10^{-3}x + 0.200$, but is equally well fit with exponential: $y=0.219e^{-0.0172x}$. Vertical and horizontal error bars for (a) and (b) are as described in Fig. 4. For (c), vertical error bars are as described in Fig. 4, horizontal error bars reflect 1 degree uncertainty in temperature control of cultures.

5. Discussion

5.1. Sr partitioning: growth rate/calcification rate vs. temperature control?

Growth rates (C-specific) and calcification rates clearly influence Sr partitioning in coccolith calcite, as observed in the tight relationships between Sr partitioning and calcification rates and estimated C incorporation rates across all investigated species at constant temperatures. Over large ranges in cell sizes, C incorporation rate, rather than cell division rate, is correlated with Sr partitioning. Over more limited ranges in cell sizes present in the same species, carbon quotas are likely to be less variable and cell division rates more correlated with C-specific growth rates. This may explain the strong correlations between cell division rate and D_{Sr} in the *G. oceanica* experiments.

The relationships between Sr partitioning and coccolithophorid calcification and growth rates are consistent with important kinetic effects on Sr partitioning documented in abiogenic calcites (Lorens, 1981). In abiogenic experiments, there is a strong linear relationship between calcite precipitation rate and D_{Sr} for precipitation rates between 30 and 3000 mg calcite/m² seed surface area/day. The coherency of the relationship between D_{Sr} and calcite production in coccoliths across all investigated species may be consistent with a conserved mechanism of calcite nucleation across all placolith-bearing coccolithophorids (Young et al., 1992). At constant temperature, calcification rate appears to be the most important control on Sr partitioning in coccolith calcites, at least in placolith-bearing heterococcoliths. Other species-specific physiological aspects of calcification must play a subordinate role in control of Sr partitioning in coccolith calcite.

Because temperature is highly correlated with growth rate and calcification rate, it is difficult to ascertain whether temperature exerts an independent influence on Sr partitioning in coccolith calcite. Temperature increases cell division rates in both temperate and Gulf Stream strains of *G. oceanica*; however, for a given temperature, growth rates are generally higher in the temperate strains. D_{Sr} vs. cell division rate shows different intercepts for the Gulf Stream and temperate strains, while D_{Sr} vs. temperature has the same relationship for both strains. The consistency of relation-

ships between D_{Sr} and calcite production across all species at constant temperature makes it difficult to invoke ecological or physiological differences to explain the different responses of Sr partitioning to cell division rate in the different strains. Nonetheless, if the Gulf stream strains were characterized by larger cells than temperate strains, it is possible that the relationship between C incorporation rate and D_{Sr} would be the same for both temperate and Gulf Stream strains and that variations in C-specific growth rate could be invoked to explain variations in D_{Sr} . The most revealing insights may come from the tropical *G. oceanica* strain, where calcite production rates were measured directly. For this strain, the slope of D_{Sr} vs. calcification rates is nearly an order of magnitude greater than that observed at constant temperature across different species. This elevated slope suggests either that temperature may exert an independent influence on Sr partitioning in coccolith calcite, or that different factors control the response of D_{Sr} to interspecific vs. intraspecific variations in calcification rate. In the experiments with *C. leptoporus* at varying temperatures, the relationship between D_{Sr} and calcification rate is comparable to that observed at constant temperatures across all species, so temperature need not be invoked to explain Sr partitioning where calcification rate varied across different species. However, the relationship between temperature and D_{Sr} is also comparable to that observed in *G. oceanica*. It is possible that the separation of calcification rate and temperature effects in the *C. leptoporus* experiments is biased by the large uncertainties in the calcite/cell for the 22 °C *C. leptoporus* experiments.

If the relationship between D_{Sr} and temperature observed in *G. oceanica* is interpreted to result primarily from variations in temperature and not from the temperature effect on calcification or growth rate, the relationship corresponds to a change in Sr/Ca ratios of 2.0% to 1.6% °C⁻¹ in the range of 15–30 °C. This is nearly an order of magnitude greater than the temperature dependence of D_{Sr} in calcite inferred from aragonite–calcite and dolomite–calcite transformation experiments (Malone and Baker, 1999). For calcification rate, the linear relationship in all species corresponds to a change in Sr/Ca ratios of 2.0% to 1.6% per 100 pg calcite/cell/day in the range of 100 to 1500 pg calcite/cell/day. This linear relationship suggests that changes in calcification rate will be

more clearly expressed in Sr partitioning in higher calcifying species. For example, at constant temperature, a 50% increase in calcification rate of typical *E. huxleyi* (28 pg calcite/cell/day) will yield less than 1% change in D_{Sr} , whereas a 50% increase in calcification rate of typical *C. leptoporus* (1200 pg calcite/cell/day) will produce a 10% change in D_{Sr} .

5.2. Prospects for paleoceanography

The possible large increase in D_{Sr} with temperature observed in these culture experiments appears to be at odds with the field study of Sr/Ca ratios of polyspecific coccolith assemblages where temperature does not appear to be the dominant control over Sr partitioning. In transects across the Equatorial Pacific upwelling front, maximum Sr/Ca ratios at the equator correspond to maximum coccolithophorid growth and calcification rates but minimum temperatures (Stoll and Schrag, 2000). The 3.5 °C temperature drop at the equator would be expected to produce up to a 6% decrease in coccolith Sr/Ca, whereas the observed 6% to 14% increase in Sr/Ca compared to Sr/Ca at 5°S and 5°N, respectively, implicates an even larger increase in calcite production rate. The dominant calcite contributor to the coccolith fraction of these sediments is *C. leptoporus* (typically 80% by weight). Since *C. leptoporus* is characterized by high calcification rates, the response of Sr partitioning to variations in calcification rate along the transect may be amplified with respect to variations in temperature. Consequently, Sr/Ca variations in coccolith sediments or fractions whose carbonate is dominated by small *G. oceanica* and *E. huxleyi* might be dominated by a temperature effect on Sr partitioning, whereas those dominated by *C. leptoporus* or *H. carterae* might be dominated by a calcification rate effect. If an independent effect of temperature on Sr partitioning could be confirmed, the Sr/Ca ratio of small placolith-bearing coccolithophorids might be a sensitive indicator of past sea surface temperature, although small changes in seawater Sr/Ca must be considered (Stoll and Schrag, 1998). Coccolith Sr/Ca (from small coccolithophorids) might have some advantages that could complement studies of foraminiferal Mg/Ca, which has recently been proposed as an indicator of past sea surface temperatures (e.g. Nürnberg et al., 1996; Lea

et al., 1999). Unlike Mg/Ca, Sr/Ca is not significantly altered by contaminating phases and Sr distribution in coccoliths is more homogeneous than in foraminifera, where calcite of different composition may be produced during different life stages. In addition, since both the small and large placolith-bearing coccolithophorids have similar depth habitats and ecology, comparison of Sr partitioning in both fractions might permit reconstruction of both past temperature and calcification rate variations. Methods to separate different coccolith species from sediments are showing promise (Stoll and Ziveri, in press; Stoll et al., 2002b).

Another potential approach to separating the temperature and calcification rate effects on Sr partitioning may be to compare coccolith Sr/Ca and Mg/Ca ratios. Mg partitioning is likely to be affected primarily by temperature and, in contrast to Sr, Mg partitioning in abiogenic calcites is not dependent on calcification rate (Morse and Bender, 1990). Thermodynamic calculations for Mg substitution in calcite (a stable solid solution series) predict that Mg/Ca should increase exponentially by about 3% °C⁻¹ between 0 and 30 °C (Lea et al., 1999 from data of Koziol and Newton, 1995). For several species of foraminifera grown in culture, Mg/Ca increases by as much as 10% °C⁻¹ (Nürnberg et al., 1996; Lea et al., 1999). It is likely that a similar dependence of Mg partitioning on temperature should exist in coccolithophorid calcite. In addition, coccolith Mg/Ca may not be affected by media pH and salinity, as is foraminiferal Mg/Ca. This is because coccolithophorids produce calcite intracellularly in an environment that must be buffered to some extent with respect to media (seawater). Lea et al. (1999) suggested that in foraminifera, the increase in Sr partitioning with temperature (1% °C⁻¹) might result from higher Mg/Ca ratios that favor Sr incorporation. Work with abiogenic calcites suggests that in the range of 2 to 10 mol% Mg, increasing incorporation of Mg favors increased Sr incorporation (Mucci and Morse, 1983). While this may be the case for foraminifera, with of 0.3 to 1.5 mol% MgCO₃ and 0.1 mol% SrCO₃, it is unclear if this mechanism would be operative at the low Mg/Ca and high Sr/Ca of coccolith calcite (0.02% MgCO₃ in some of our cultures; Stoll et al., 2001). Regardless, if Mg partitioning reflects temperature variation, and Sr partitioning reflects both variation in temperature and

calcification rates, combined measurements may permit resolution of both factors.

6. Conclusions

Five common placolith-bearing coccolithophorid algae were cultured to investigate controls on coccolith Sr. Sr incorporation in coccolith calcite varied by over 30% in these experiments, and is enhanced at rapid calcification rates and at higher temperature. At constant temperature, Sr partitioning is linearly related to calcification rates over the entire range of species studied, consistent with a conserved mechanism for calcite nucleation across all placolith-bearing coccolithophorids suggested by Young et al. (1992, 1999). This relationship is also consistent with kinetic effects on Sr partitioning in abiogenic calcites (Lorens, 1981). Because this relationship is linear, a proportional change in calcification should be expressed much more strongly in the D_{Sr} of large species with rapid calcite production than in smaller species, which produce calcite more slowly. Consequently, efforts to utilize coccolith Sr/Ca in sediments to estimate past variations in coccolithophorid calcification rate should focus on the larger placolith-bearing species. Experiments with several strains of *G. oceanica* suggest that temperature may increase D_{Sr} by up to 2% to

1.6% °C⁻¹ in the range of 15 to 30 °C. Consequently, temperature changes could contribute significantly to variations in coccolith Sr/Ca in marine samples. It may be possible to separate these influences on coccolith Sr/Ca by separately analyzing Sr/Ca in species that produce calcite rapidly and those that produce calcite slowly, if both undergo comparable relative changes in calcification rates. Analysis of coccolith Mg/Ca may also help distinguish the relative importance of temperature and calcification rate effects on coccolith Sr/Ca since temperature is likely to be the primary control on coccolith Mg/Ca.

Acknowledgements

This material is based upon work supported by the North Atlantic Treaty Organization under a Grant awarded in 1998 (DGE-98-04555 to HMS) and by the II Plan Regional de Investigacion del Principado de Asturias (HMS), and by the EC-TMR project CODENET—Coccolithophorid Evolutionary Biodiversity and Ecology Network (FRMX-ET97-0113). We thank Larry Brand for assistance in collecting Gulf Stream *G. oceanica* isolates, Hanno Kinkel for valuable discussions and a careful reading of this manuscript, and Harry Elderfield and Dirk Nürnberg for thoughtful reviews.

Appendix A. Origin of strains cultured in this study

Strain ID	Species	Isolated from	Date	Cultured at
A4725	<i>G. oceanica</i>	Gulf Stream, Florida, USA	4/97	ETH
A4727	<i>G. oceanica</i>	Gulf Stream, Florida, USA	4/97	ETH
ARC3	<i>G. oceanica</i>	Atlantic Shelf, France	6/98	ETH
ESP 186	<i>G. oceanica</i>	Western Mediterranean, Spain	2/98	ETH
JS8	<i>G. oceanica</i>	Southern Mediterranean	5/98	ETH
PC71	<i>G. oceanica</i>	Atlantic Shelf, Portugal	7/98	ETH
PC11M2	<i>C. leptoporus</i>	Atlantic Shelf, Portugal	7/98	ETH
PC6	<i>C. leptoporus</i>	Atlantic Shelf, Portugal	7/98	ETH
PC131	<i>C. leptoporus</i>	Atlantic Shelf, Ireland	7/98	ETH
MS1	<i>E. huxleyi</i>	North Sea	98	Caen
JS1 A	<i>G. oceanica</i>	Southern Mediterranean	5/98	Caen
KL2	<i>C. pelagicus</i>	Atlantic Shelf, France	12/99	Caen
PC11M3 B	<i>C. leptoporus</i>	Atlantic Shelf, Portugal	7/98	Caen
ASM 36	<i>U. sibogae sibogae</i>	Western Mediterranean (Alboran Sea)	10/99	Caen
ESP6 M1	<i>U. sibogae foliosa</i>	Western Mediterranean, Spain	4/99	Caen

Appendix B

Cultured at	Sample type	Species	Strain	Day of culture	Nutrients (if not <i>f/2</i>)	Exper. no.	Temp.	Growth phase (harvested)	Cells/ml (at harvest)	Weighted average (Sr/Ca media)	D_{Sr} (corr. for media Sr/Ca)	D_{Sr} (no corr. for media Sr/Ca)	Media pH
ETH	lith	<i>C. leptoporus</i>	PC131				21.2	exp	44453	8.76	0.378	0.388	
ETH	lith	<i>C. leptoporus</i>	PC6				17.0	exp	66328	8.83	0.336	0.347	
ETH	lith	<i>C. leptoporus</i>	PC6				17.0	exp	66328	8.83	0.336	0.347	
ETH	lith	<i>C. leptoporus</i>	PC6				21.2	exp	52500	8.79	0.367	0.378	
ETH	filter	<i>C. leptoporus</i>	PCIIIM2			-3	17.0	exp	14375	8.65	0.356	0.360	
ETH	filter	<i>C. leptoporus</i>	PCIIIM2			-2	17.0	exp	18594	8.67	0.356	0.361	
ETH	filter	<i>C. leptoporus</i>	PCIIIM2			-1	17.0	exp	22656	8.70	0.351	0.357	
ETH	filter	<i>C. leptoporus</i>	PCIIIM2			-1	17.0	exp	44063	8.78	0.347	0.356	
ETH	filter	<i>C. leptoporus</i>	PCIIIM2			-3	17.0	exp	68242	8.82	0.351	0.362	
ETH	filter	<i>C. leptoporus</i>	PCIIIM2			-2	17.0	exp	86198	8.83	0.350	0.362	
ETH	lith	<i>C. leptoporus</i>	PCIIIM2				21.2	exp	42567	8.77	0.364	0.373	
ETH	lith	<i>C. leptoporus</i>	PCIIIM2				21.2	exp	42567	8.77	0.363	0.372	
ETH	filter	<i>G. oceanica</i>	A4725			-1-2	30.2	exp	292778	8.72	0.347	0.354	
ETH	filter	<i>G. oceanica</i>	A4725			-2-1	30.2	exp	180000	8.65	0.354	0.358	
ETH	lith	<i>G. oceanica</i>	A4725			-1/2	30.2	exp	103333	8.61	0.366	0.368	
ETH	lith	<i>G. oceanica</i>	A4725			-1/2	30.2	exp	103333	8.61	0.363	0.366	
ETH	lith	<i>G. oceanica</i>	A4725			-2-1	30.2	exp	110000	8.61	0.366	0.368	
ETH	lith	<i>G. oceanica</i>	A4727			1	17.0	exp	228889				
ETH	lith	<i>G. oceanica</i>	A4727			-2	17.0	exp	331333	8.66	0.284	0.288	
ETH	lith	<i>G. oceanica</i>	A4727			-1	22.0	exp	111667	185.51	0.333	0.333	
ETH	lith	<i>G. oceanica</i>	A4727			-2	22.0	exp	224167	185.51	0.326	0.326	
ETH	filter	<i>G. oceanica</i>	A4727			2	21.2	exp	83744	8.59	0.331	0.333	
ETH	filter	<i>G. oceanica</i>	A4727			2	21.2	exp	474815	8.80	0.357	0.368	
ETH	lith	<i>G. oceanica</i>	A4727			1	21.2	exp	111667	8.61	0.331	0.333	
ETH	lith	<i>G. oceanica</i>	A4727			2	21.2	exp	224167	8.67	0.322	0.326	
ETH	lith	<i>G. oceanica</i>	A4727		<i>f/20</i>		30.2	exp	110000	8.62	0.369	0.372	
ETH	lith	<i>G. oceanica</i>	A4727			-2/2-3	30.2	exp	161111	8.65	0.404	0.408	
ETH	filter	<i>G. oceanica</i>	A4727			-3-2	30.2	exp	219630	8.69	0.361	0.366	
ETH	lith	<i>G. oceanica</i>	A4727			-3/2	30.2	exp	299167	8.74	0.364	0.372	
ETH	lith	<i>G. oceanica</i>	ARC3			-1	17.0	exp	234306	8.79	0.287	0.295	
ETH	lith	<i>G. oceanica</i>	ARC3			-2	17.0	exp	303056	8.84	0.284	0.294	
ETH	lith	<i>G. oceanica</i>	ARC3			-3	17.0	exp	163889	8.73	0.292	0.298	
ETH	lith	<i>G. oceanica</i>	ARC3		<i>f/20</i>		21.2	exp	245000	8.73	0.331	0.338	
ETH	lith	<i>G. oceanica</i>	ARC3		<i>f/20</i>		21.2	stat	341111	8.76	0.307	0.314	

ETH	lith	<i>G. oceanica</i>	ARC3	$f/200$	-1		exp	26953				
ETH	lith	<i>G. oceanica</i>	ARC3	$f/200$	-2		exp	28281				
ETH	lith	<i>G. oceanica</i>	ARC3		-1	21.2	exp	151667	8.67	0.324	0.328	
ETH	lith	<i>G. oceanica</i>	ARC3		-3	21.2	exp	206111	8.71	0.327	0.333	
ETH	lith	<i>G. oceanica</i>	ARC3			26.1	exp	200000	8.68	0.341	0.346	
ETH	lith	<i>G. oceanica</i>	ESP186		-1	17.0	exp	140556	8.68	0.312	0.317	
ETH	lith	<i>G. oceanica</i>	ESP186		-2	17.0	exp	161389	8.70	0.304	0.309	
ETH	lith	<i>G. oceanica</i>	ESP186		-3	17.0	exp	195278	8.72	0.315	0.322	
ETH	lith	<i>G. oceanica</i>	ESP186		-1+	21.2	exp	1157778	8.24	0.000	0.325	
ETH	lith	<i>G. oceanica</i>	ESP186			26.1	exp	200000	8.70	0.367	0.374	
ETH	lith	<i>G. oceanica</i>	JS8		-1	17.0	exp	169167	8.72	0.296	0.302	
ETH	lith	<i>G. oceanica</i>	JS8		-2	17.0	exp	298611	8.81	0.299	0.308	
ETH	lith	<i>G. oceanica</i>	JS8		-3	17.0	exp	314444	8.81	0.302	0.311	
ETH	lith	<i>G. oceanica</i>	JS8		-2	21.2	exp	337222	8.70	0.329	0.335	
ETH	lith	<i>G. oceanica</i>	JS8			26.1	exp	200000	9.05	0.335	0.355	
ETH	lith	<i>G. oceanica</i>	PC71		-2	17.0	exp	229444	8.71	0.286	0.291	
ETH	lith	<i>G. oceanica</i>	PC71		-3	17.0	exp	167778	8.68	0.297	0.301	
ETH	lith	<i>G. oceanica</i>	PC71		-1	21.2	exp	386111	8.82	0.315	0.325	
ETH	lith	<i>G. oceanica</i>	PC71		-2	26.1	exp	389444	9.05	0.349	0.370	
Caen	lith	<i>E. huxleyi</i>	MS1	3	A3	17.0	exp	445333	8.58	0.299	0.300	7.69
Caen	lith	<i>E. huxleyi</i>	MS1	6	A6	17.0	exp-stat	1914400	8.69	0.286	0.291	8.14
Caen	lith	<i>E. huxleyi</i>	MS1	10	A10	17.0	stat	1906333	8.72	0.284	0.290	8.46
Caen	lith	<i>E. huxleyi</i>	MS1	14	A14	17.0	stat	1853366	8.72	0.286	0.292	8.36
Caen	lith	<i>G. oceanica</i>	JS1 A	6	B6	17.0	exp	453000	8.79	0.296	0.305	7.63
Caen	lith	<i>G. oceanica</i>	JS1 A	10	B10	17.0	stat	335667	8.71	0.289	0.295	7.93
Caen	lith	<i>G. oceanica</i>	JS1 A	18	B18	17.0	stat	279333	8.71	0.286	0.292	7.80
Caen	lith	<i>C. pelagicus</i>	KL2	3	C3	17.0	exp	8483	8.57	0.339	0.339	
Caen	lith	<i>C. pelagicus</i>	KL2	6	C6	17.0	exp	64400	8.68	0.337	0.342	7.47
Caen	lith	<i>C. pelagicus</i>	KL2	10	C10	17.0	stat	71917	8.69	0.329	0.334	7.82
Caen	lith	<i>C. pelagicus</i>	KL2	18	C18	17.0	stat	63667	8.68	0.333	0.338	7.42
Caen	lith	<i>C. leptoporus</i>	PC11M3B	3	D3	17.0	exp	18283	8.63	0.314	0.317	
Caen	lith	<i>C. leptoporus</i>	PC11M3B	6	D6	17.0	exp	57367	8.70	0.306	0.311	7.50
Caen	lith	<i>C. leptoporus</i>	PC11M3B	10	D10	17.0	exp-stat	160667	8.71	0.304	0.310	8.10
Caen	lith	<i>C. leptoporus</i>	PC11M3B	18	D18	17.0	stat	156000	8.72	0.303	0.309	7.79
Caen	lith	<i>U. sibogae sibogae</i>	ASM36	3	E3	17.0	exp	6833	8.55	0.283	0.283	
Caen	lith	<i>U. sibogae sibogae</i>	ASM36	6	E6	17.0	exp	16066	8.56	0.273	0.273	7.76
Caen	lith	<i>U. sibogae sibogae</i>	ASM36	10	E10	17.0	stat	43567	8.60	0.242	0.243	8.09
Caen	lith	<i>U. sibogae sibogae</i>	ASM36	18	E18	17.0	stat	45083	8.60	0.257	0.259	8.70
Caen	lith	<i>U. sibogae foliosa</i>	ESP6M1	3	F3	17.0	exp	25117	8.59	0.289	0.291	
Caen	lith	<i>U. sibogae foliosa</i>	ESP6M1	6	F6	17.0	exp	88800	8.66	0.285	0.288	7.53
Caen	lith	<i>U. sibogae foliosa</i>	ESP6M1	10	F10	17.0	exp-stat	255667	8.77	0.266	0.273	7.96
Caen	lith	<i>U. sibogae foliosa</i>	ESP6M1	18	F18	17.0	stat	341333	8.78	0.261	0.268	7.80

References

- Archer, D., Winguth, A., Lea, D., Mahowald, N., 2000. What caused the glacial/interglacial $p\text{CO}_2$ cycles? *Rev. Geophys.* 38, 159–189.
- Broerse, A.T.C., 2000. Coccolithophore export production in selected ocean environments: seasonality, biogeography and carbonate production. PhD Dissertation, Vrije Universiteit, Amsterdam, 185 pp.
- Brownlee, C., Nimer, N., Dong, L.F., Merrett, J.M., 1994. Cellular regulation during calcification in *Emiliania huxleyi*. In: Green, J.C., Leadbeater, B.S.C. (Eds.), *The Haptophyte Algae: Systematics Association Special Volume No. 51*. Clarendon Press, Oxford, pp. 133–148.
- deVrind-deJong, E.W., Van Emburg, P.R., deVrind, J.P.M., 1994. Mechanisms of calcification: *Emiliania huxleyi* as a model system. In: Green, J.C., Leadbeater, B.S.C. (Eds.), *The Haptophyte Algae. Systematics Association Special Volume No. 51*. Clarendon Press, Oxford, pp. 149–166.
- Dong, L.F., Nimer, N.A., Okus, E., Merrett, M.J., 1993. Dissolved inorganic carbon utilization in relation to calcite production in *Emiliania huxleyi* (Lohmann) Kamptner. *New Phytol.* 123, 679–684.
- Fernandez, E., Marañón, E., Balch, W.M., 1996. Intracellular carbon partitioning in the coccolithophorid *Emiliania huxleyi*. *J. Mar. Syst.* 9, 57–66.
- Guillard, R.R.L., 1975. Culture of phytoplankton for feeding marine invertebrates. In: Smith, W.L., Chanley, M.H. (Eds.), *Culture of Marine Vertebrate Animals*. Plenum, New York, pp. 29–60.
- Jasper, J.P., Hayes, J.M., 1990. A carbon isotope record of CO_2 levels during the late Quaternary. *Nature* 347, 462–464.
- Jasper, J.P., Hayes, J.M., Mix, A.C., Prahl, F.G., 1994. Photosynthetic fractionation of ^{13}C and concentrations of dissolved CO_2 in the central equatorial Pacific during the last 255,000 years. *Paleoceanography* 9, 781–798.
- Keller, M.D., Selvin, R.C., Claus, W., Guillard, R.R.L., 1987. Media for the culture of oceanic ultraphytoplankton. *J. Phycol.* 23, 633–638.
- Klaas, C., Bollman, J., Probert, I., Thierstein, H., in preparation. Morphological and physiological characterization of *Gephyrocapsa oceanica*: an experimental approach.
- Kozioł, A.M., Newton, R.C., 1995. Experimental determination of the reactions magnesite + quartz = periclase + CO_2 and the enthalpies of formation of enstatite and magnesite. *Am. Mineral.* 80, 1252–1260.
- Lea, D.W., Mashioita, T.A., Spero, H.J., 1999. Controls on magnesium and strontium uptake in planktonic foraminifera determined by live culturing. *Geochim. Cosmochim. Acta* 63, 2369–2379.
- Lorens, R.B., 1981. Sr, Cd, Mn, and Co distribution coefficients in calcite as a function of calcite precipitation rate. *Geochim. Cosmochim. Acta* 45, 553–561.
- Malone, M.J., Baker, P.A., 1999. Temperature dependence of the strontium distribution coefficient in calcite: an experimental study from 40° to 200° and application to natural diagenetic calcites. *J. Sediment. Res.* 69, 216–223.
- Morse, J.W., Bender, M.L., 1990. Partition coefficients in calcite: examination of factors influencing the validity of experimental results and their application to natural systems. *Chem. Geol.* 82, 265–277.
- Mucci, A., Morse, J.W., 1983. The incorporation of Mg^{+2} and Sr^{+2} into calcite overgrowths: influence of growth rate and solution composition. *Geochim. Cosmochim. Acta* 47, 217–233.
- Nimer, N.A., Merrett, M.J., 1992. Calcification and utilization of inorganic carbon by the coccolithophorid *Emiliania huxleyi* Lohmann. *New Phytol.* 121, 173–177.
- Nürnberg, D., Bijma, J., Hemleben, C., 1996. Assessing the reliability of magnesium in foraminiferal calcite as a proxy for water mass temperatures. *Geochim. Cosmochim. Acta* 60, 803–814.
- Prahl, F.G., Wakeham, S.G., 1987. Calibration of unsaturated patterns in long-chain ketone compositions for paleotemperature assessment. *Nature* 330, 367–369.
- Riegman, R., Stolte, W., Noordeloos, A.A.M., 1998. A model system approach to biological climate forcing: the example of *Emiliania huxleyi*. Final Report Subproject (b): Physiology, Nederlands Instituut voor Onderzoek der Zee, 32 pp.
- Stoll, H.M., Schrag, D.P., 1998. Effects of Quaternary sea level changes on strontium in seawater. *Geochim. Cosmochim. Acta* 62, 1107–1118.
- Stoll, H.M., Schrag, D.P., 2000. Coccolith Sr/Ca as a new indicator of coccolithophorid calcification and growth rate. *Geochem., Geophys., Geosystems* 1, 1–24.
- Stoll, H.M., Ruiz-Encinar, J., Garcia-Alonso, J.I., Rosenthal, Y., Klaas, C., Probert, I., 2001. A first look at paleotemperature prospects from Mg in coccolith carbonate: cleaning techniques and culture measurements. *Geochemistry, Geophysics, Geosystems* 8 May 2001.
- Stoll, H.M., Rosenthal, Y., Falkowski, P., 2002a. Climate proxies from Sr/Ca of coccolith calcite: calibrations from continuous culture of *Emiliania huxleyi*. *Geochim. Cosmochim. Acta* 66, 927–936.
- Stoll, H.M., Ziveri, P., Geisen, M., Probert, I., Young, J.R., 2002b. Potential and limitations of Sr/Ca ratios in coccolith carbonate: new perspectives from cultures and monospecific samples from sediments. *Philos. Trans. R. Soc. London A* 360, 719–747.
- Stoll, H.M., Ziveri, P., in press. Separation of monospecific and restricted coccolith assemblages from sediments using differential settling velocity. *Marine Micropaleontology*.
- Takahashi, K., 1994. Coccolithophorid biocoenosis: production and fluxes to the deep sea. In: Green, J.C., Leadbeater, B.S.C. (Eds.), *The Haptophyte Algae*. Clarendon Press, Oxford, pp. 335–350.
- Tesoriero, A.J., Pankow, J.F., 1996. Solid solution partitioning of Sr^{2+} , Ba^{2+} , and Cd^{2+} to calcite. *Geochim. Cosmochim. Acta* 60, 1053–1063.
- Watson, E.B., 1996. Surface enrichment and trace-element uptake during crystal growth. *Geochim. Cosmochim. Acta* 60, 5013–5020.
- Westbroek, P., Byddemeier, B., Coleman, M., Dok, D.J., Fautin, D., Stal, L., 1994. Strategies for the study of climate forcing by calcification. In: Doumenge, F. (Ed.), *Past and Present Biomineralization Processes. Considerations about the Carbonate Cycle*. Bulletin de l'Institut océanographique, Monaco, vol. 13, pp. 37–60.

- Young, J.R., 1994. Functions of coccoliths. In: Winter, A., Siesser, W. (Eds.), *Coccolithophorids*. Cambridge Univ. Press, Cambridge, pp. 63–82.
- Young, J.R., Ziveri, P., 2000. Calculation of coccolith volume and its use in calibration of carbonate flux estimates. *Deep-Sea Res., Part 2, Top. Stud. Oceanogr.* 47 (9–11), 1679–1700.
- Young, J.R., Didymus, J.M., Bown, P.R., Prins, B., Mann, S., 1992. Crystal assembly and phylogenetic evolution in heterococcoliths. *Nature* 356, 516–518.
- Young, J.R., Davis, S.A., Bown, P.R., Mann, S., 1999. Coccolith ultrastructure and biomineralisation. *J. Struct. Biol.* 126, 195–215.